

# DEVELOPMENT OF DENSE CERAMIC MEMBRANES FOR HYDROGEN SEPARATION

U. (Balu) Balachandran, T. H. Lee, S. Wang, and S. E. Dorris  
Energy Technology Division, Argonne National Laboratory, Argonne, IL 60439

K. S. Rothenberger  
National Energy Technology Laboratory, Pittsburgh, PA 15236

## ABSTRACT

Novel cermet (i.e., ceramic-metal composite) membranes have been developed for separating hydrogen from gas mixtures at high temperature and pressure. The hydrogen permeation rate in the temperature range of 600-900°C was determined for three classes of cermet membranes (ANL-1, -2, and -3). Among these membranes, ANL-3 showed the highest hydrogen permeation rate, with a maximum flux of 5.9 cm<sup>3</sup>(STP)/min-cm<sup>2</sup> for a 0.1-mm-thick membrane at 900°C. The effects of membrane thickness and hydrogen partial pressure on permeation rate indicate that the bulk diffusion of hydrogen is rate-limiting for ANL-3 membranes >0.1 mm thick, but kinetic limitations due to interfacial effects are expected at some lower, currently unknown, thickness. The lack of degradation in permeation rate during exposure to a simulated syngas mixture suggests that ANL-3 membranes are chemically stable and suitable for long-term applications.

## INTRODUCTION

The U.S. Department of Energy's Office of Fossil Energy sponsors a wide variety of research, development, and demonstration programs that will maximize the use of vast domestic fossil resources and ensure a fuel-diverse energy sector while responding to global environmental concerns. Development of cost-effective membrane-based reactor and separation technologies is of significant interest for applications in advanced fossil-based power and fuel technologies. Because concerns over global climate change are driving nations to reduce CO<sub>2</sub> emissions, hydrogen is considered the fuel of choice for the electric power and transportation industries. Although it is likely that renewable energy sources will ultimately be used to generate hydrogen, fossil-fuel-based technologies will supply hydrogen in the interim.

As part of the effort to devise cost-effective, efficient processes for producing and utilizing hydrogen, Argonne National Laboratory (ANL) and the National Energy Technology Laboratory (NETL) are developing dense, hydrogen-permeable membranes. Dense membranes made from palladium were developed elsewhere and have been commercially available since the early 1960's, but they are expensive and are limited to operating temperatures below ≈600°C [1]. The goal at ANL/NETL is to develop a dense, ceramic-based membrane that is highly selective, like palladium-based membranes but is less expensive and chemically stable in corrosive environments at operating temperatures up to ≈900°C. To be commercially viable, a membrane should provide a hydrogen flux of ≈10 cm<sup>3</sup>(STP)/min-cm<sup>2</sup> with a pressure drop of ≈1 atm across the membrane [2]. From the outset, the effort at ANL/NETL has focused on

BaCe<sub>0.8</sub>Y<sub>0.2</sub>O<sub>3-δ</sub> (BCY), which is a mixed proton/electron conductor with a high total electrical conductivity [3, 4] and therefore may yield a high hydrogen flux without the need for electrodes or electrical circuitry. Despite its high total electrical conductivity, however, the electronic component of the conductivity of BCY is insufficient to support a high nongalvanic hydrogen flux [5, 6]. To increase the electronic conductivity, and thereby increase the hydrogen flux, we have developed various cermet (i.e., ceramic-metal composite) membranes, in which 40 vol.% of a metal is dispersed in a ceramic matrix [7, 8].

The cermet membranes are classified as ANL-1, -2, or -3, on the basis of the hydrogen transport properties of the metal and matrix phases. In ANL-1 membranes, a metal with low hydrogen permeability is distributed in the hydrogen-permeable matrix of BCY. ANL-2 membranes also contain the hydrogen-permeable BCY matrix, but they contain a hydrogen transport metal, i.e., a metal with high hydrogen permeability. In ANL-3 membranes, a metal with high hydrogen permeability is dispersed in a ceramic matrix of low hydrogen permeability, e.g., Al<sub>2</sub>O<sub>3</sub> or BaTiO<sub>3</sub>. Each membrane is identified by a number and a letter, where the number represents the class of membrane as described above, and the letter indicates a specific combination of metal and matrix phases. For example, ANL-3a is an ANL-3 membrane that contains "metal-a" in a matrix of Al<sub>2</sub>O<sub>3</sub>, whereas ANL-3b contains a different combination of hydrogen transport metal and ceramic. When general comments are made about an entire class of membranes, e.g., ANL-3 membranes, a letter is not included in the description.

The first class of membranes, ANL-1, contained a metal with low hydrogen permeability in a hydrogen-permeable matrix, BCY. Hydrogen permeation through ANL-1a was higher than that in monolithic BCY because the metal increased the overall electronic conductivity of the membrane; hydrogen diffusion through the metal phase was negligible because of its low hydrogen permeability. To increase the hydrogen flux through the membrane, we developed ANL-2a, in which the metal of ANL-1a was replaced by a hydrogen transport metal. This metal facilitated hydrogen diffusion through BCY by increasing the overall electronic conductivity and it provided an alternative path for hydrogen diffusion. Although BCY and the metal phase both contribute to hydrogen permeation through ANL-2 membranes, most of the hydrogen diffuses through the metal and only a small amount diffuses through BCY [9]. Because BCY contributes relatively little to the overall permeation rate of ANL-2 membranes, exhibits poor mechanical properties, and is chemically unstable under some conditions of interest, we developed ANL-3 membranes. In ANL-3 membranes, the BCY matrix of ANL-1 and -2 membranes is replaced by a ceramic with superior mechanical properties and thermodynamic stability, e.g., Al<sub>2</sub>O<sub>3</sub> or ZrO<sub>2</sub>, to form a membrane with a high hydrogen permeation rate, but with higher strength and greater chemical stability.

In this paper, we discuss the state of development of the various cermet membranes (ANL-1, -2, and -3) and compare their hydrogen permeation rates. The effects of membrane thickness, temperature, and hydrogen partial pressure on the permeation flux of ANL-3 are presented. The results of the hydrogen permeation measurements in simulated synthesis gas (i.e., "syngas") are also shown as an indication of probable membrane behavior under actual operating conditions.

## EXPERIMENTAL

BCY powder was prepared at ANL as previously described [5]. All membranes were prepared to contain 40 vol.% metal phase. BCY and metal powders were mixed together to

prepare powders for ANL-1a and -2a membranes. Powders for ANL-3b and -3d membranes were prepared by mixing one of two hydrogen transport metals with ceramic powders that are reported to be poor proton conductors [10]. Powders were pressed uniaxially to prepare disks ( $\approx 22$  mm in diameter  $\times$  2 mm thick) for sintering.

Sintering conditions for the various membranes were selected on the basis of their composition. ANL-1a and -2a membranes were sintered for 5 h in 4%  $H_2$ /balance Ar at  $1420^\circ C$ . ANL-3b membranes were sintered at  $1350^\circ C$  for 12 h in air, whereas ANL-3d membranes were sintered in air for 5 h at  $1390^\circ C$ .

To test permeation, a sintered disk was polished with 600-grit SiC polishing paper and then affixed to an  $Al_2O_3$  tube that was part of the assembly shown in Fig. 1. A seal formed when the assembly was heated to  $950^\circ C$  and spring-loaded rods squeezed a gold ring between the membrane and the  $Al_2O_3$  tube. One side of the sample was purged with 4%  $H_2$ /balance He during sealing, while the other side was purged with 100 ppm  $H_2$ /balance  $N_2$ . The leakage rate following this procedure was typically  $<10\%$  of the total permeation flux.

The flow rate of sweep gas during permeation measurements (100 ppm  $H_2$ /balance  $N_2$ ) was controlled with a mass flow controller (MKS) and was measured with a flow calibrator (Field-Cal 570 from Humonics). The sweep gas was analyzed with a Hewlett-Packard 6890 gas chromatograph (GC). Feed gases included 100%  $H_2$ , simulated syngas (66%  $H_2$ , 33% CO, and 1%  $CO_2$ ), and "dry" or "wet" 4%  $H_2$ /balance He. For wet feed gas, 4%  $H_2$ /balance He was bubbled through a water bath at room temperature to give  $\approx 0.03$  atm  $H_2O$ ; for the dry condition, 4%  $H_2$ /balance He was introduced directly into the furnace from the gas cylinder.

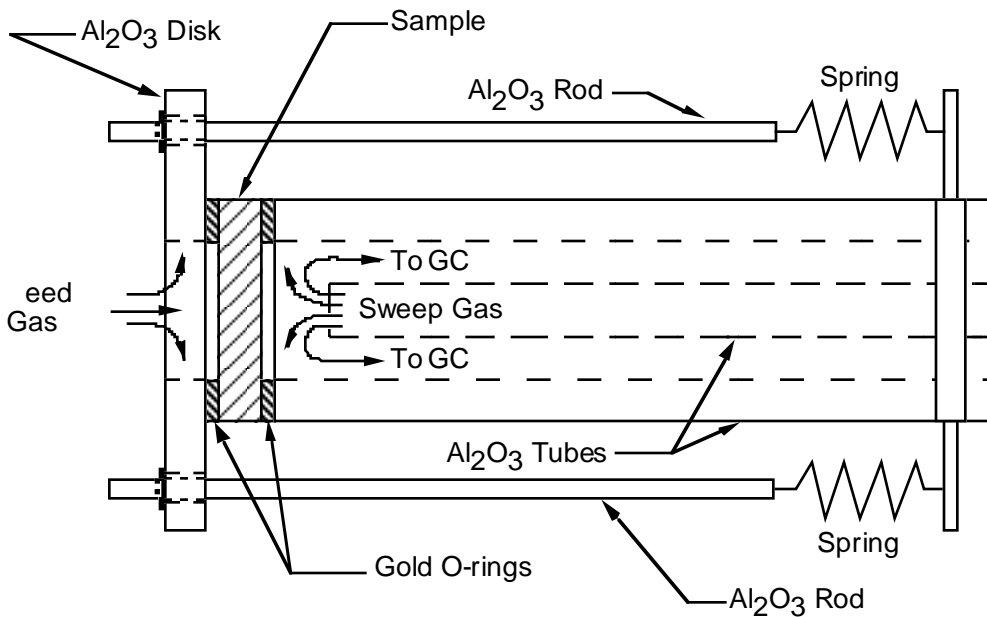


Figure 1. Experimental assembly for measuring hydrogen flux. GC = gas chromatograph.

## RESULTS

The hydrogen permeation rates for ANL-1a, -2a, and -3b are compared in Fig. 2 for a feed gas of 4% H<sub>2</sub>/balance He. The thicknesses of the membranes are normalized to the thickness for ANL-1a, i.e., 0.50 mm, to allow direct comparison of permeation properties. The original thickness of each membrane is shown in the inset in Fig. 2. In as much as the measurement conditions were the same, the permeation rates for the various samples can be compared directly. Among these membranes, ANL-3b exhibited the highest permeation rate, which was approximately three times higher than that of ANL-1a over the whole temperature range. When compared with ANL-2a, the permeation rate for ANL-3b was  $\approx 35\%$  higher at 900°C and  $\approx 80\%$  higher at 600°C. ANL-3b exhibited the highest permeation rate because the hydrogen permeability of its metal phase is the highest of the various metals used to date.

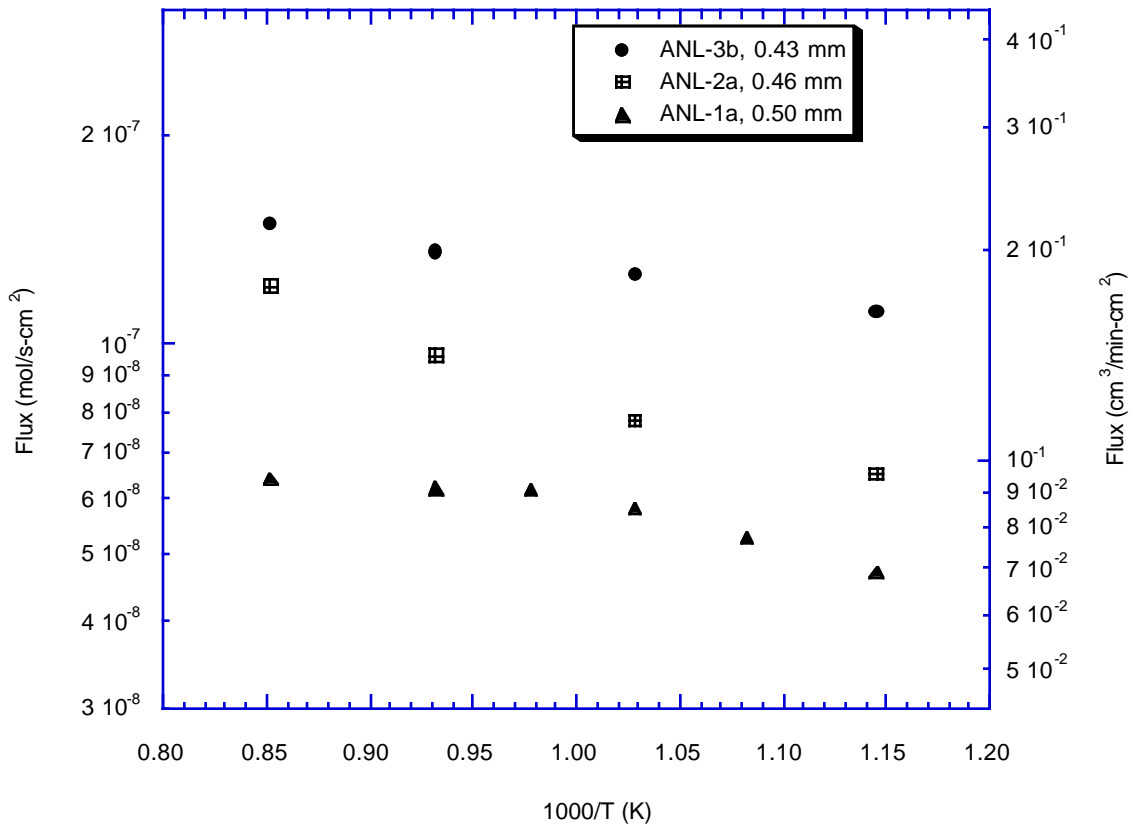


Figure 2. Hydrogen permeation rates through ANL-1a, -2a, and -3b when wet 4% H<sub>2</sub>/balance He was feed gas. Thicknesses are normalized to 0.5 mm; original thickness of each membrane shown on inset.

Figure 3 shows the temperature and thickness dependence of the hydrogen flux through ANL-3b when wet 100% H<sub>2</sub> was used as the feed gas. Because the leakage at lower temperatures was high, permeation flux for 0.1-mm-thick membrane is shown at only 900°C, where maximum flux of 5.9 cm<sup>3</sup>/min-cm<sup>2</sup> was achieved. With either 100% H<sub>2</sub> (Fig. 3) or 4% H<sub>2</sub>/balance He as the feed gas, the hydrogen permeation rate increased with temperature and was proportional to the inverse of membrane thickness over the whole temperature range. This finding indicates that bulk diffusion of hydrogen is rate-limiting for thicknesses >0.1 mm, and that reducing membrane thickness can increase permeation flux.

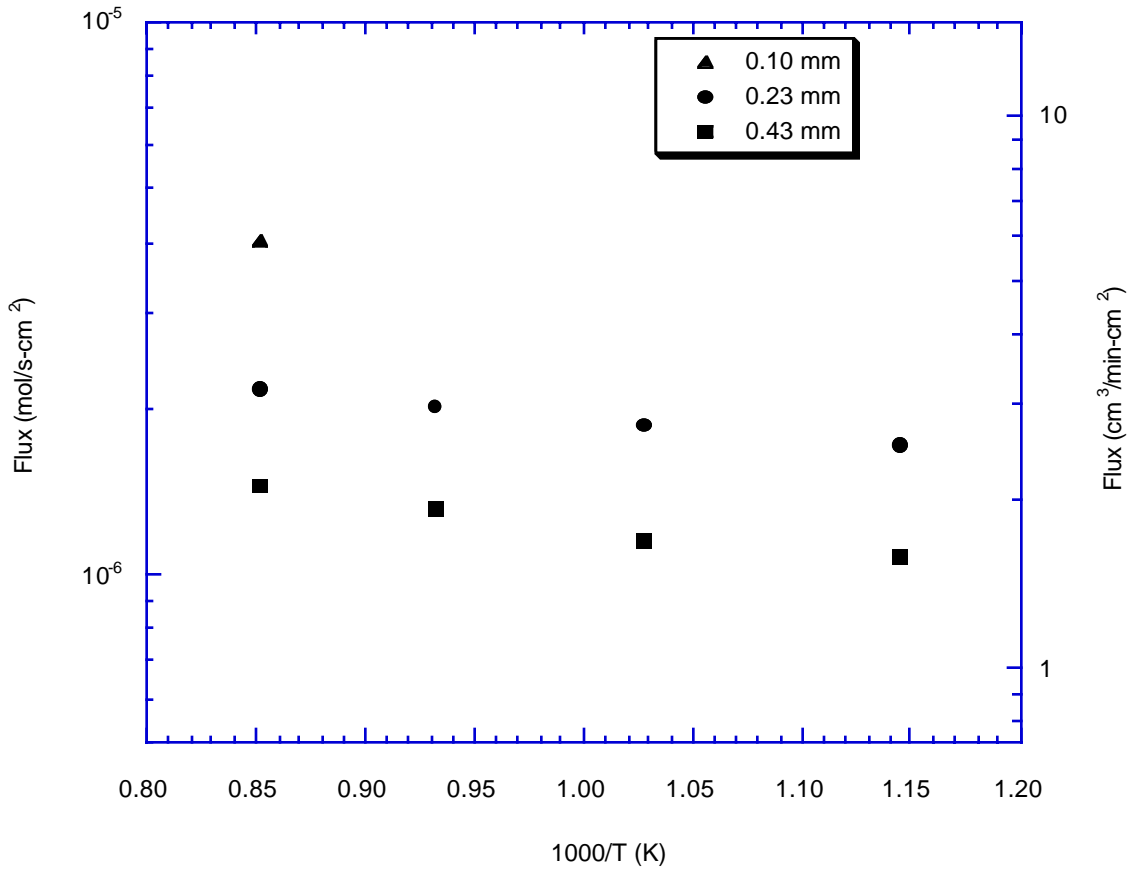


Figure 3. Hydrogen permeation rate through 0.10-, 0.23- and 0.43-mm-thick ANL-3b when feed gas was wet 4% H<sub>2</sub>/balance He.

The effect of hydrogen partial pressure on hydrogen flux is shown in Fig. 4 for 0.23-mm-thick ANL-3b at 800 and 900°C. In the figure, hydrogen permeation flux is plotted as a function of the difference in square root of hydrogen partial pressure for the feed and sweep sides of the membrane. At both temperatures, the flux varies linearly with the difference in square root of hydrogen partial pressure, which is characteristic of bulk-limited hydrogen diffusion through metals [11]. These results confirm that, in this thickness range, the bulk

diffusion of hydrogen through the metal phase dominates the hydrogen flux through ANL-3b. At some lesser thickness, however, interfacial reactions may become rate-limiting.

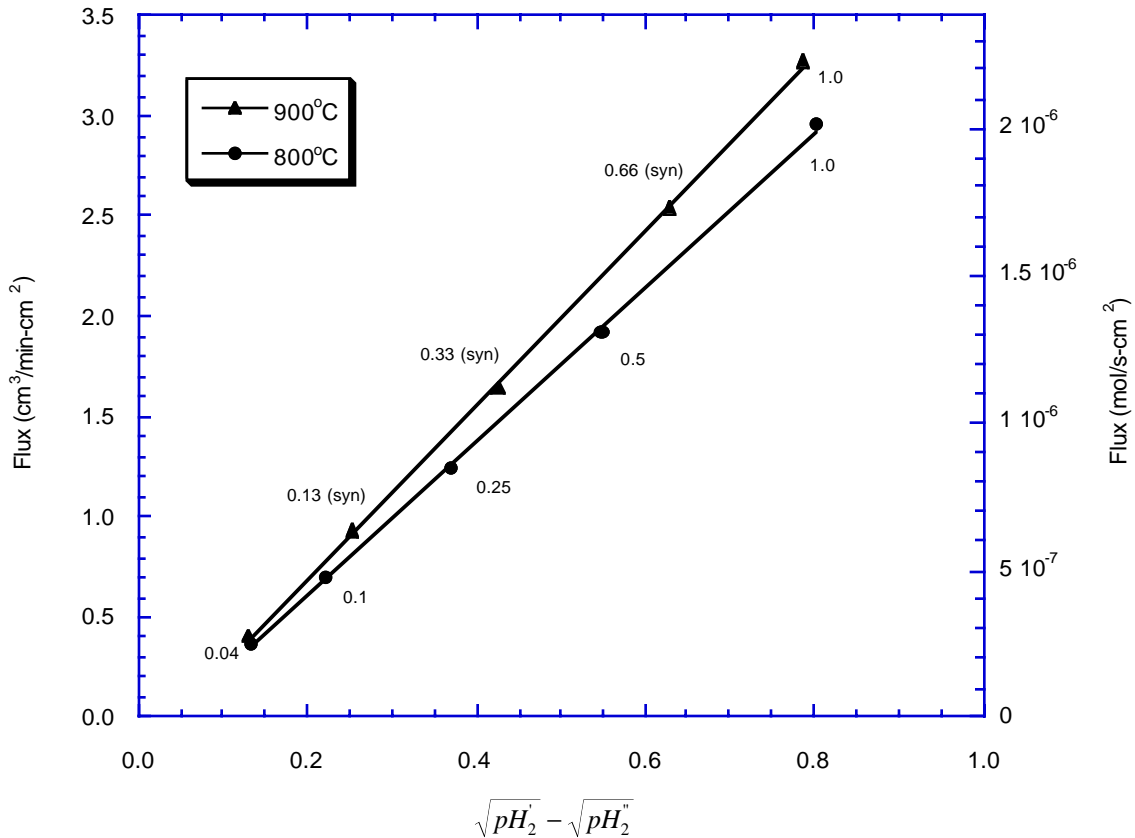


Figure 4. Dependence of hydrogen permeation rate on partial pressure of hydrogen ( $pH_2$ ) for ANL-3b (thickness = 0.23 mm).  $pH_2' = pH_2$  of feed gas;  $pH_2'' = pH_2$  of sweep gas;  $pH_2$  of feed gas indicated on figure; (syn) = gas mixtures made with simulated syngas.

The chemical stability of ANL-3b in syngas was tested by measuring its hydrogen flux at several temperatures for times up to 190 h. The results obtained from a 0.43-mm-thick membrane are shown in Fig. 5. A feed gas of 4%  $H_2$ /balance He was flowed before and after exposure to syngas at each temperature, and the leakage rate of hydrogen was estimated by measuring the helium concentration in the sweep gas. No helium leakage was measured at any of the temperatures. As seen in Fig. 5, no noticeable decrease in flux was observed during up to 190 h of operation at each temperature. Likewise, similar tests with 0.23-mm-thick ANL-3b showed no decrease in the hydrogen flux during 120 h of exposure to syngas at 900°C.

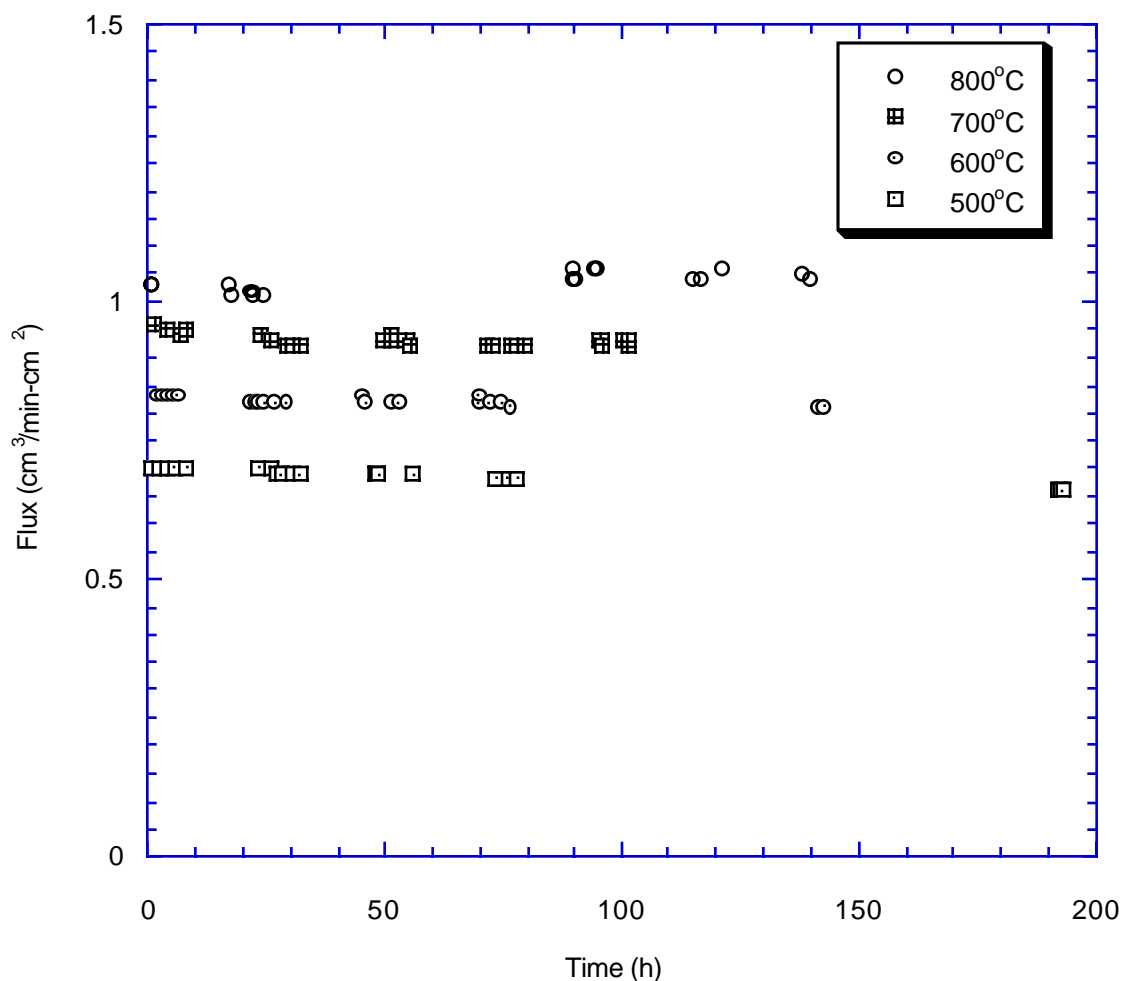


Figure 5. Hydrogen permeation rate through ANL-3b (0.43-mm-thick) vs. time in simulated syngas (66% H<sub>2</sub>, 33% CO, and 1% CO<sub>2</sub>) at various temperatures.

The ceramic matrix of ANL-3b, BaTiO<sub>3</sub>, is a convenient matrix, because its sintering temperature is relatively low when compared with that of Al<sub>2</sub>O<sub>3</sub>. Al<sub>2</sub>O<sub>3</sub>, on the other hand, is stronger and exhibits better structural reliability. To improve the structural reliability of thin ANL-3 membranes, we developed ANL-3d, in which ANL-3b metal is dispersed in a matrix of Al<sub>2</sub>O<sub>3</sub> matrix instead of BaTiO<sub>3</sub>. Because the melting point of the metal phase in ANL-3b is relatively lower than the sintering temperature of Al<sub>2</sub>O<sub>3</sub>, we could not obtain dense membranes. With a sintering aid, however, we sintered >95%-dense ANL-3d membranes at 1390°C. Handling of the ANL-3d membrane during its preparation for permeation measurements demonstrated qualitatively that it was significantly stronger and harder than ANL-3b. Figure 6 shows that the permeation properties of ANL-3d are nearly the same as those of ANL-3b. The

thickness of ANL-3d, 0.53 mm, was normalized to the thickness for ANL-3b, 0.43 mm, to directly compare their permeation properties. The similarity in permeation rates indicates that the sintering aid did not degrade the properties of the hydrogen transport metal.

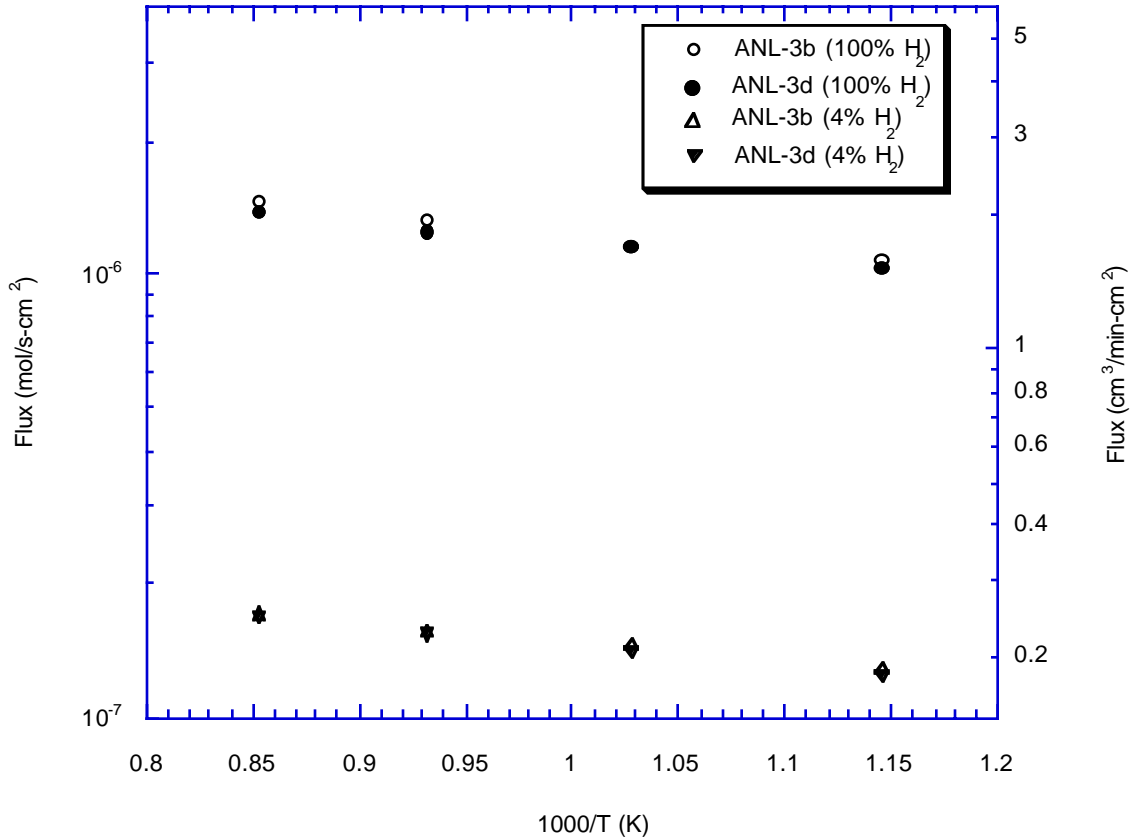


Figure 6. Hydrogen permeation rates of ANL-3b and -3d membranes when feed gas was 4% H<sub>2</sub> and 100% H<sub>2</sub>. The membrane thickness of ANL-3d (0.53 mm) was normalized to that for ANL-3b (0.43 mm) to allow direct comparison of permeation properties.

The Al<sub>2</sub>O<sub>3</sub> matrix of ANL-3d is chemically more stable than the BCY matrix of ANL-2a in a harsh environment that contains high concentrations of CO<sub>2</sub>. This is seen in Fig. 7, where the permeation rate through the two membranes is shown as a function of time during exposure at 900°C to a dry syngas of composition 2.0% CH<sub>4</sub>, 19.6% H<sub>2</sub>, 19.6% CO, and 58.8% CO<sub>2</sub> (mol.%). The permeation rate through ANL-2a decreased dramatically after only several minutes, whereas the hydrogen flux through ANL-3d was stable for >3 h. Examination of the ANL-2a surface by scanning electron microscopy after the permeation measurements showed that the BCY matrix had decomposed to form BaCO<sub>3</sub> and other phases. These results show that a chemically stable matrix such as Al<sub>2</sub>O<sub>3</sub> or ZrO<sub>2</sub> will be required for application of the membrane in atmospheres with high CO<sub>2</sub> concentrations.

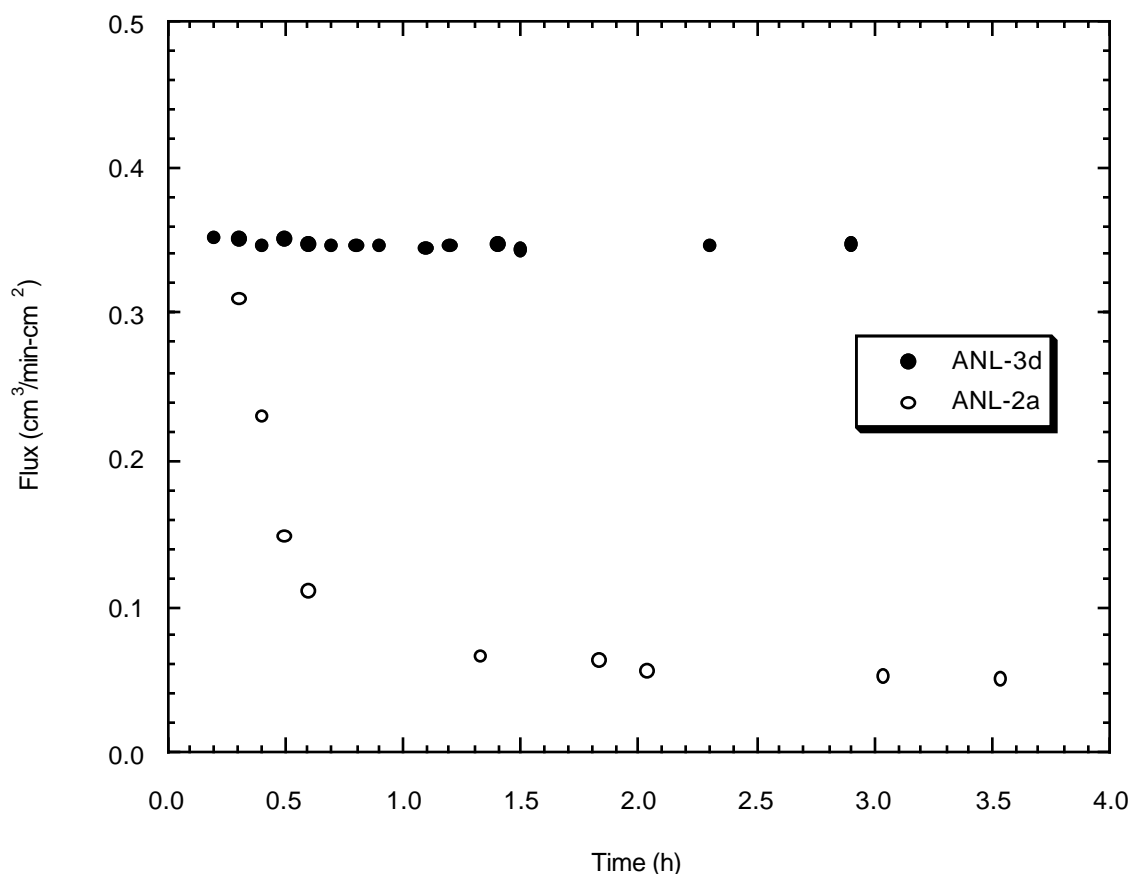


Figure 7. Permeation rate through Al<sub>2</sub>O<sub>3</sub>-based ANL-3d and BCY-based ANL-2a in a feed gas containing 2.0% CH<sub>4</sub>, 19.6% H<sub>2</sub>, 19.6% CO, and 58.8% CO<sub>2</sub> (mol.%). Thickness of ANL-3d membrane was 0.53 mm; thickness of ANL-2a, 0.43 mm.

## CONCLUSIONS

We have developed cermet membranes that nongalvanically separate hydrogen from gas mixtures. The highest measured hydrogen flux was 5.9 cm<sup>3</sup>/min-cm<sup>2</sup> for an ANL-3b membrane at 900°C. For ANL-3 membranes with thicknesses of 0.1-0.5 mm, permeation rate is limited by the bulk diffusion of hydrogen through the metal phase. The effect of hydrogen partial pressure on permeation rate confirmed this conclusion and indicates that higher permeation rates can be obtained by decreasing the membrane thickness. Permeation rate in a syngas atmosphere for times up to 190 h showed no degradation in performance, which suggests that ANL-3 membranes may be suitable for long-term, practical hydrogen separation.

## ACKNOWLEDGMENTS

This work has been supported by the U.S. Department of Energy, National Energy Technology Laboratory, under Contract W-31-109-Eng-38.

## REFERENCES

- [1]. S. Uemiya, Separation and Purification Methods, 28(1), 51 (1999).
- [2]. S. Benson, Ceramics for Advanced Power Generation, IEA Coal Research 2000, London, UK., pp.43.
- [3]. H. Iwahara, T. Yajima, and H. Uchida, Solid State Ionics, 70/71, 267 (1994).
- [4]. H. Iwahara, Solid State Ionics, 77, 289 (1995).
- [5]. J. Guan, S. E. Dorris, U. Balachandran, and M. Liu, Solid State Ionics, 100, 45 (1997).
- [6]. J. Guan, S. E. Dorris, U. Balachandran, and M. Liu, J. Electrochem. Soc., 145, 1780 (1998).
- [7]. J. Guan, S. E. Dorris, U. Balachandran, and M. Liu, Ceram. Trans., 92, 1 (1998).
- [8]. U. Balachandran, T. H. Lee and S. E. Dorris, in Proc. 16th Annual International Pittsburgh Coal Conf., Pittsburgh, PA, Oct. 11-15, 1999, Pittsburg Coal Conf. Pittsburgh, PA.
- [9]. U. Balachandran, T. H. Lee, G. Zhang, S. E. Dorris, K. S. Rothenberger, B. H. Howard, B. Morreale, A. V. Cugini, R. V. Siriwardane, J. A. Poston Jr., and E. P. Fisher, in Proc. 26th Intl. Technical Conf. on Coal Utilization and Fuel Systems, Clearwater, FL, Mar. 5-8, 2001, Coal Technical Association, Gaithersburg, MD. pp. 751-761.
- [10]. K.-D. Kreuer, Chem. Mater., 8, 610 (1996).
- [11]. R. E. Buxbaum and T. L. Marker, J. Membr. Sci., 85, 29 (1993).